Feasible Time and Energy Optimal, Minimum Oscillations Trajectory Design

- Application to 3D Cranes and Multi-rotor Unmanned Aerial Vehicles

Attila Nemes

Óbuda University, Doctoral School of Safety and Security Sciences, Bécsi út 96/b, H-1034 Budapest, Hungary

nemesa@stud.uni-obuda.hu

Abstract: In this paper a novel trajectory design method is presented, which is capable of generating real-time parametrisations to any point-to-point path curve, while guaranteeing trajectory feasibility, time and energy efficiency – feasible optimality. To validate my results the proposed new design method is applied to a 3D overhead crane and a multi-rotor unmanned aerial vehicle trajectory planning. The 3D overhead crane is a simple system, which can very notably present system oscillations. Multi-rotors like quad- and hexa-rotors are popular and well-studied mobile robots, being representatives of unmanned aerial vehicles (UAVs), since they are relatively simple to build and easy to control, while being of versatile applicability, capable of vertical take-off and landing; still their efficient and precise control is a formidable challenge. My approach is to first have a proper quality, feasible trajectory planned, so then the control problem is simplified. Capability of real time trajectory generation is a must for autonomous systems, while preventing oscillations, minimising the control effort, and at the same time also minimising the required time to complete the displacement are practical issues, which are all in focus of this research paper.

Keywords: real-time; feasible time and energy efficient; oscillation reduction; trajectory design; 3D overhead cranes; mobile robots; multi-rotors; quad- and hexa-rotors; unmanned aerial vehicles

1 Introduction

Small model vehicles including quadrotor unmanned aerial rotorcrafts are harder to control than the full sized real vehicles as the models have significantly lower mass thus, lower inertia, which induces much shorter time constants. On the other hand up scaled 3D cranes are the most obvious tools to present systems state oscillations. Optimal trajectory design is a still challenging task, though it is usually considered well formulised since Pontryagin's work in the early '60s Control mechanisms as PID, back stepping (computed torque) and their fuzzy variants have been also well studied and successfully used for decades on many systems including multi-rotors [1].

Benchmarking and qualitative evaluation of different autonomous quadrotor flight controllers was presented in [2]. Three characteristic representatives of frequently used flight control techniques were considered: PID, back stepping and fuzzy. Dynamic performances, trajectory tracking precision, energy efficiency and control robustness upon stochastic internal and/or external perturbation was considered. Two experimental scenarios were constructed for a characteristic benchmarking procedure: dynamic quadrotor flight in a 3D loop manoeuvre and a typical cruising flight along the trajectory introduced by setting waypoints with pre-defined GPS coordinates. Through analysing simulation results the back stepping method presented the best control performances in sense of trajectory tracking precision. The other two algorithms had presented slightly better characteristics in sense of energy efficiency, they had lower energy consumption. By increasing the flight speed dynamic effects become influential on the system performances: the back stepping method was more sensitive to increased flight speeds than the PID and the fuzzy logic controller – as studied in [2]. When reading the analysis one can notice the dominant chattering characteristics of actuator signals, obviously the system has significant difficulties in precisely tracing the designated trajectory. Can this only be contributed to control algorithm deficiency, or the trajectory itself is not appropriate? Since all three control algorithms are mature, proven on many real life and simulation environments, it is more probable that the prescribed trajectory is not suitable for multi-rotors.

Anti-swing control of cranes is still a popular research subject, since their construction simplicity, thus availability along wide industrial practical applicability. Very advanced control mechanisms, including input shaping have been studied; the primary goal is to move the pendulum like system efficiently, keeping the pendulum system oscillations at minimum, so that the payload mass swing – trajectory tracking error is at minimum [3].

Both these research fields have a clear conclusion for me: the state space trajectory has to be more carefully designed than connecting control points of desired body position coordinates.

In the second paragraph this paper will present a brief summary of optimal trajectory designs currently used in literature. In the third paragraph a summary of all relevant multi-rotor subsystems and their characteristics will be presented, their transient behaviours analysed, also a simple 3D overhead crane model will be cited. The proposal of this paper – trajectory design for oscillations sensitive systems like multi-rotors and cranes - is presented in the fourth paragraph. The fifth paragraph presents the algorithm, and highlights the difficulties of its implementation for discreet sampling time environments. The sixth paragraph presents application results for a multi-rotor and a crane trajectory example. The seventh paragraph describes the usability of the proposed trajectory generation method, it also presents the applicability of this method to other electrically actuated system, and points out how the basic approach of this proposal can be applied to other systems of different actuator types. In the final paragraph conclusions are drawn and possible future work is outlined.

2 Overview of Optimal Trajectory Design Methods

The basic problem to solve is moving a body of mass m from point A to point B. In general there are set boundaries on the trajectory in terms of allowed geometrical regions or obstacles, velocity, acceleration or even jerk (third time derivative of displacement) limits are defined. Usually time optimality and/or energy optimality requirements are associated with a planned movement along a chosen path. The pure theoretical approach starts with finding possible 3D geometric path curves from A to B. The exact time optimal solution is then selecting the shortest geometric displacement curve s and traveling along this path with v_{max} the maximum allowed velocity for the shortest time period of $t_f = s/v_{max}$. For moving a body of mass m, such a time optimal trajectory, where an instant jump-start is demanded with v_{max} maximum speed from point A, and then it is planned to have an abrupt stop to zero velocity at time t_f in point B is, is just physically not feasible; obviously there has to be an acceleration and a deceleration period – we cannot physically generate mathematical Dirac force impulses having extremely precise integral value. This realization was adopted in „bang-bang" trajectory plans – see Figure 1, where the first part of the trajectory was planned for a_{max} constant maximal acceleration until reaching v_{max}, then traveling with v_{max} for the appropriate distance, and finally decelerating with a constant maximal deceleration $-a_{max}$ to reach the target. These "bang-bang" trajectories were dubbed „time optimal" trajectories, though obviously for $a_{max} = v_{max}/(t_f/2)$ we get $\sqrt{s/a_{max}} > s/v_{max}$ .These „bang-bang" trajectories imply that we plan for using discontinuous force actions $F(t_0) = 0$, then in the next infinitesimally close time $F(t_0 + \varepsilon) = F_{max} = m \cdot a_{max}$; also when reaching the target it plans for an instant drop from $F(t_f - \varepsilon) = F_{max}$ to $F(t_f) = 0$, which is also not feasible in real life for non-rigid bodies. For these trajectories the best we can do is to apply fast and strong enough control loops so that the controlled system transient period is acceptably small, while the overshoot and the settling time also remains "controlled" – as obviously these trajectories induce vibrations, significant system state oscillations. Well noticeable are the immense energy spikes used for achieving these fast discontinuous transients, compensating for overshoots and the resulting vibrations, oscillations after the rise time – be it mechanical or electrical in nature. These effects are unwanted – they increase wear and reduce the life span of physical systems and in extreme cases they are source of catastrophic accidents. Vibrations are also highly undesirable for precise path tracking. Be it cranes or robotic manipulators (RMs) – the lowest vibration levels were identified to correspond to the magnitude of the second time derivative of the induced torque, while an appropriately constructed trajectory can decrease oscillations and energy consumption by a factor of 10, – as in [4].

Soon after introducing trajectory planning, it had been realised that also the control effort can and should be minimised. First minimum acceleration trajectories had been devised, and then the cost function had been adopted to include the direct control energy effort. In [5] Pontryagin defined the notion of mathematical theory of optimal processes. To minimize the total used energy E_{t_f} of moving mass m from A to B, a cost function like $E_{t_f} = \int_0^{t_f} \boldsymbol{P_{abs}}(t)dt$ is devised by cumulating the absolute value of the instantaneous applied power $\boldsymbol{P_{abs}}(t) = |\boldsymbol{F}(t)\boldsymbol{v}(t)| + |\boldsymbol{\tau}(t)\boldsymbol{\omega}(t)|$ through which the product of the absolute acceleration and velocity function profile of the shortest geometric path is minimized. Since $\boldsymbol{P_{abs}}(t) = \sum_i m_i \cdot |\boldsymbol{a_i}(t)| \cdot \boldsymbol{v_i}(t)$ this minimization process is very similar to looking for the minimal jerk trajectory, only that here we are actually looking for a kind of minimal acceleration trajectory, which results in a polynomial trajectory of order 3, with a discontinuity in acceleration for $t = 0$ and $t = t_f$. Still system vibrations remained to be a substantial issue. Research had pointed out that vibrations are in correlation with the jerk. The first derivative of acceleration, which is the third time derivative of the displacement is called jerk $\boldsymbol{j} = d^3\boldsymbol{s}/dt^3 = \dddot{\boldsymbol{s}}(t)$. Polynomial trajectories of order 5 can be constructed as minimum jerk trajectories – as in Figure 1, got constructed by minimization of a cost function like $\boldsymbol{C}(s) = \frac{1}{2}\int_0^{t_f} \dddot{\boldsymbol{s}}(t)^2 dt$. Calculus of variation or Hamiltonian with Lagrange functions is the usual tool to solve this mathematical problem, where a perturbation function $\boldsymbol{\delta}(t)$ is added with a constant multiplier α in the form of $\boldsymbol{s}(t) + \alpha \cdot \boldsymbol{\delta}(t)$, such that for boundary conditions the perturbation and its derivatives are 0 like $\boldsymbol{\delta}(x) = \dot{\boldsymbol{\delta}}(x) = \ddot{\boldsymbol{\delta}}(x) = \dddot{\boldsymbol{\delta}}(x) = 0$ for $x = 0$ and $x = t_f$. Based on calculus of variations instead of minimizing $\boldsymbol{C}(\boldsymbol{s}(t) + \alpha \cdot \boldsymbol{\delta}(t)) = \frac{1}{2}\int_0^{t_f}(\dddot{\boldsymbol{s}}(t) + \alpha \cdot \dddot{\boldsymbol{\delta}}(t))^2 dt$ the zero point of its partial derivative for $\alpha = 0$ is calculated like $\partial \boldsymbol{C}(s + \alpha\delta)/\partial\alpha|_{\alpha=0} = \int_0^{t_f}\left(\dddot{\boldsymbol{s}}(t) + \alpha \cdot \dddot{\boldsymbol{\delta}}(t)\right) \cdot \dddot{\boldsymbol{\delta}}(t)dt\Big|_{\alpha=0} = \int_0^{t_f} \dddot{\boldsymbol{s}}(t) \cdot \dddot{\boldsymbol{\delta}}(t)dt$. Using boundary conditions the result is $-\int_0^{t_f} \boldsymbol{s}^{(\boldsymbol{6})}(t) \cdot \boldsymbol{\delta}(t)dt = 0$, which according to the calculus of variations is equivalent to the requirement of having the sixth derivative of the displacement equal to zero: $\boldsymbol{s}^{(\boldsymbol{6})}(t) = 0$.

Knowing the boundary conditions of the trajectory $\boldsymbol{s}(x) = \dot{\boldsymbol{s}}(x) = \ddot{\boldsymbol{s}}(x)$ at $x = 0, x = t_f$ the a, b, c, d, e parameters can be calculated as a polynomial trajectory $\boldsymbol{s}(t) = a + bt + ct^2 + dt^3 + et^4 + ft^5$, $\dot{\boldsymbol{s}}(t) = b + 2ct + 3dt^2 + 4et^3 + 5ft^4$, $\ddot{\boldsymbol{s}}(t) = 2c + 6dt + 12et^2 + 20ft^3$.

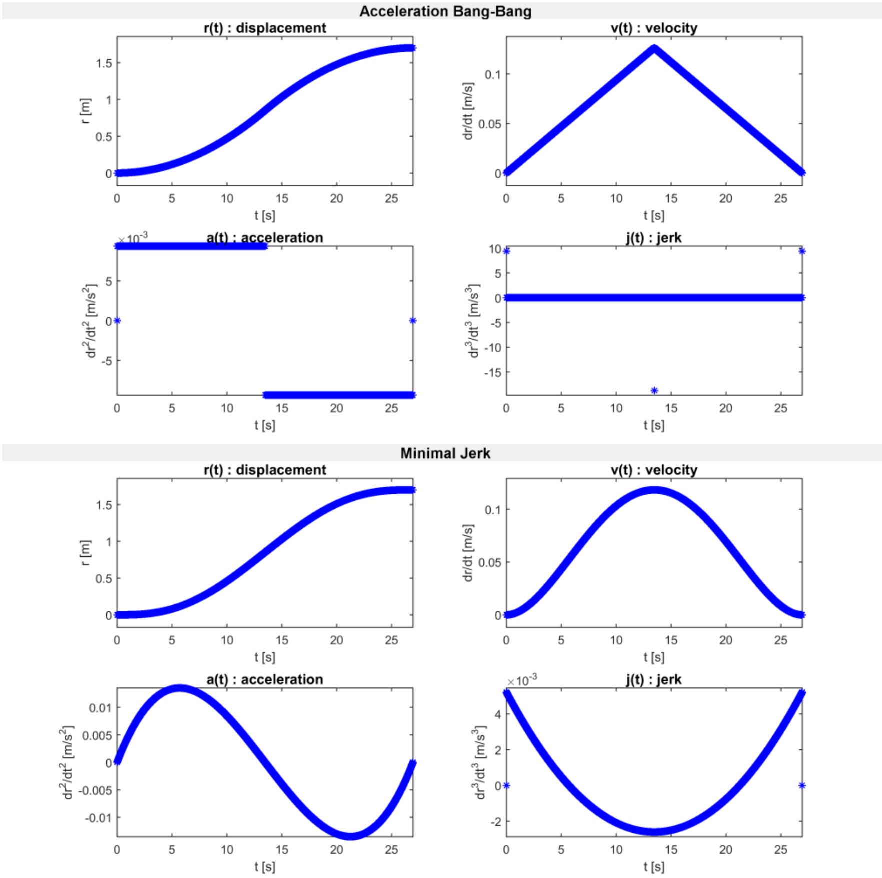

Figure 1

Acceleration bang-bang; and minimal jerk trajectory components

For such trajectories jerk $\boldsymbol{j}(t_0) = \dddot{\boldsymbol{s}}(t = 0) = 6d$, obviously start with an instantaneous jump from 0 to $6d$, also at the final moment $t = t_f$ there is a jump from a non-zero to 0 jerk value. As we have previously discussed: this induces oscillations. A sudden jerk induces vibrations; in case of vehicles like elevators, high speed trains, roller-coasters the ride is very uncomfortable at those points.

Notice that the control signal (commonly the torque output of an electric motor) is not a virtual mathematical quantity to be optimised without constraints. The actuators are real physical systems. Even for the simplest direct electro-motor actuator considering $\boldsymbol{i}_e(t) \cong const_1 \cdot \boldsymbol{\tau}(t) = const_2 \cdot \boldsymbol{a}(t)$ model the discontinuity in jerk means a discontinuity in $d\boldsymbol{i_e}(t)/dt$ that translates to voltage $\boldsymbol{u_e}(t)/dt$ discontinuity, which is not possible, since in an electro-motor the armature voltage depends on $d\boldsymbol{i_e}(t)/dt$. Also if we accept the paradigm of not planning for a discontinuity of the second derivative of the linear displacement (acceleration), we have to accept the same for the rotation displacement as well, and we have $d\boldsymbol{i_e}(t)/dt = 1/K_\tau \cdot (J_m\ddot{\boldsymbol{\omega}} + \mu_m\dot{\boldsymbol{\omega}})$, where $\boldsymbol{\omega}(t)$ is the rotation speed, the time derivative of the rotor position, K_τ is the torque constant, J_m is the motor inertia, and μ_m is the rotor friction coefficient..

For electro-motor torque actuated mechanical systems like common cranes, RMs or multi-rotor UAVs cost functions like $E_{t_f} = \int_0^{t_f} \boldsymbol{\tau_{abs}}(t)dt$ are also used to minimize the total torque, the used actuator electric energy; as in a stationary state of the actuators it is common to use a simplified motor torque model, where the applied current is linearly proportional to the resulting torque $\boldsymbol{i_e}(t) \cong const \cdot \boldsymbol{\tau}(t)$ [6]. The dynamic model of an RM has a quite complex torque equation like $\boldsymbol{\tau}(\mathrm{t}) = \boldsymbol{H}(\boldsymbol{q}) \cdot \ddot{\boldsymbol{q}} + \dot{\boldsymbol{q}}^T \cdot \boldsymbol{C}(\boldsymbol{q}, \dot{\boldsymbol{q}}) \cdot \dot{\boldsymbol{q}} + \boldsymbol{G}(\boldsymbol{q})$, with highly nonlinear $\boldsymbol{H}(\boldsymbol{q}), \boldsymbol{C}(\boldsymbol{q}), \boldsymbol{G}(\boldsymbol{q})$ functions, where joint variables $\boldsymbol{q} = \boldsymbol{q}(s)$ themselves are not trivially deducted through the systems construction geometry along the end effector path $\boldsymbol{s}$, so solutions to energy optimal trajectories come only either in flavours of drastic reductions to linear approximations of the RM dynamics, or in flavours of numerical iterative methods. In the end linear approximation results for RMs are in general sub-optimal, while numerical iterative solutions are far from real time usability. Vibration levels in RMs have been identified as induced even by discontinuities in the second derivative of the torque, this must not come as a surprise as $\ddot{\boldsymbol{\tau}}(t) \cong const_1 \cdot \ddot{\boldsymbol{i}}_{\boldsymbol{e}}(t) \cong const_2 \cdot d^2(\boldsymbol{\omega}(t)^2)/dt = const_2 \cdot (2\dot{\boldsymbol{\omega}}^2 + 2\boldsymbol{\omega}\ddot{\boldsymbol{\omega}})$. We have the angular position of the actuator rotor, which is a real physical body with mass that cannot be accelerated in a discontinuous manner. The most simple and obvious way to present (trajectory induced) system oscillations is to analyse a up-scaled crane system – with a longer pendulum length, so that all oscillation sings are notably present as either the payload trajectory tracking error or in the state space rate of change; for a crane it is the second time derivative of payload position that will magnify the presence of trajectory induced oscillations in a feed forward control system.

My major point is that limiting the actuator torque vibration must not be considered only as a mathematical problem of limiting $|\ddot{\boldsymbol{q}}|$. It is time to realize that in trajectory planning not the extent of discontinuity in a physical quantity is the problem, but the existence of a discontinuity itself is unacceptable or at least sub-optimal approach.

Researches like [7] and [8] are pointing out that applying input shaping instead of direct step change, for example in BLDC rotor speed control, results in both the unwanted oscillations reduction and the energy consumption reduction; also the responsiveness of the system can be increased - when there are no current spikes, much less energy used [9].

The pioneering work of [10] relying on [5] presents a time optimal trajectory design method for RMs, which accounts for pre-defined torque limits, while the optimisation problem is transferred to the trajectory space, as torque limits are transformed to acceleration limits. The path ***f(s)*** describes the position of the end effector in the task coordinates, the state variables became parameterised functions $\boldsymbol{q} = \boldsymbol{f}(s), \dot{\boldsymbol{q}} = \boldsymbol{f}'(s)\dot{s}, \ddot{\boldsymbol{q}} = \boldsymbol{f}''(s)\dot{s}^2 + \boldsymbol{f}'(s)\ddot{s}$. For the class of nonlinear plants which can be decoupled by state variable feedback - as cranes, RMs and multi-rotor UAVs - finding optimal trajectories becomes equivalent to finding the appropriate parametrisation *s* for ***f(s)***, given the pre-defined feasibility limits on torque in system dynamic equations.

There are multiple approaches for multi-rotor UAV trajectory planning, starting from simple path plotting up to complete trajectory generation: [11], [12], [13]. [14] describe the possibility of defining the major path milestones by visual fuzzy servoing, also any map based three search algorithm can be applied to define the next major target point during a flight mission. To facilitate both time and energy efficiency of flight the major path milestones are best connected with continuous curvature functions ***f(s)*** [15].

3 Overview of Multi-Rotor UAV Flight Dynamics

Multi-rotors like quad- and hexa-rotors are popular representatives of UAVs as they are relatively simple to build and easy to control, while being of versatile applicability, capable of vertical take-off and landing. Also the multi-rotor architecture has simple mechanics, high relative payload capability and good manoeuvrability. The study of multi-rotor kinematics and dynamics is based on the physics of aerial platforms [16]. The kinematics with the general force and torque dynamics of any symmetric multi-rotor (quad- or hexa- rotors) is the equivalent 6DOF dynamic system of mass *m* moved against the gravity acceleration *g*. Generalised translational forces: $m\left(\ddot{\boldsymbol{\xi}} + g[0\ 0\ 1]^T\right) = \boldsymbol{F}_\xi$; and the generalised body torques are:

$$\boldsymbol{J}(\boldsymbol{q})\ddot{\boldsymbol{q}} + \boldsymbol{C}(\boldsymbol{q}, \dot{\boldsymbol{q}})\dot{\boldsymbol{q}} = \boldsymbol{\tau_B}, \tag{1}$$

where in analogy with robotic manipulators: $\boldsymbol{J}\ddot{\boldsymbol{q}}$ is the inertia matrix; $\boldsymbol{C}\dot{\boldsymbol{q}}$ is the Coriolis term;and the state vector $\boldsymbol{q}$ is composed of the Euler angles for roll, pitch and jaw $\boldsymbol{q} = [\boldsymbol{\phi}, \boldsymbol{\theta}, \boldsymbol{\psi}]$. The roll and pitch of a multi-rotor UAV can be calculated from the path curve vector function as ***(x(t),y(t),z(t))*** and the required yaw motion ***ψ(t)*** as presented in [14] like:

$$\boldsymbol{\phi} = asin\left(\frac{\dot{x}sin\psi - \dot{y}cos\psi}{\ddot{x}^2 + \ddot{y}^2 + (\ddot{z}+g)^2}\right), \boldsymbol{\theta} = atan\left(\frac{\dot{x}cos\psi - \dot{y}sin\psi}{(\ddot{z}+g)}\right) \tag{2}$$

Minimum-snap polynomial (***x,y,z***) trajectories are proven good for quadrotors, “since the motor commands and attitude accelerations of the vehicle are proportional to the snap, or forth derivative, of the path” [17]. In [17] the rotor blade velocity is considered as an arbitrary control input. As 7th order minimum-snap polynomial trajectories are discontinuous in displacement crackle, fifth derivative of displacement, my claim is that this is still a sub-optimal approach; again: the rotor blade velocity is not an arbitrary theoretical control signal, but a real, electro-mechanical physical system, subject to aero dynamical load conditions.

The goal of this paper is to present a new method for flexible and efficient real-time direct path parametrisation, which is capable of generating physically feasible, time-and energy optimal, bounded, continuous trajectories with minimal induced oscillations; a method even usable for autonomous navigation. The notion of time and energy optimality is not used in mathematics theory manner, but in real life, physically feasible engineering manner. The process of finding optimal trajectories is here focused on finding the appropriate parametrisation for the path vector function ***f(t)***, given the pre-defined feasibility limits on the displacement time derivatives, in conjunction with the effects of the path curvature. The defined boundary conditions of the trajectory have to be satisfied. The defined limits on maximum values for arbitrary time derivatives of the displacement have to be obeyed. Continuity and smoothness of every trajectory component has to be ensured up to the predetermined order: 6 times smooth in case of multi-rotors, 4 times smooth in case of cranes and RMs. As described in [18] and [19], to have realistic, feasible torques along a trajectory, which are efficiently controllable without chattering, we need smooth torque changes. For indirect rotor-blade propulsion systems (ships, multi-rotors) we have the propulsion motor force or torque $\boldsymbol{M_M}(t) \approx const \cdot \boldsymbol{\omega}(t)^2$ proportional to the square of the rotor angular velocity. The applied mechanical force or torque $\boldsymbol{M_B}(t) \approx m * \ddot{\boldsymbol{\mu}}(t)^2$ excreted onto the body is proportional with the second derivative of the linear position or rotation angle $\ddot{\boldsymbol{\mu}}(t)$ of the body. As the body is driven by a rotor blade, $\boldsymbol{\omega}(t)$ is proportional to $\ddot{\boldsymbol{\mu}}$, the body angular acceleration. In reality no discontinuities can physically occur, not even in third time derivatives of a displacement neither for the controlled system, nor for the control actuator.

Multi-rotor UAVs introduce yet another layer of complexity: their torque dynamics is similar to RMs, while they are propelled by a lift force of rotating blades fixed to the body $\vec{z}$ axes. Paths $[\boldsymbol{\xi}(t), \boldsymbol{\mu}(t)] = \left[\left(\boldsymbol{x}(t), \boldsymbol{y}(t), \boldsymbol{z}(t)\right), \boldsymbol{\psi}(t)\right]$ defined along earth coordinate $\vec{x}, \vec{y}, \vec{z}$ axes extended with the desired jaw rotation angle $\psi(t)$ translate to body rotation coordinates $\boldsymbol{\mu}(t) = \left(\boldsymbol{\varphi}(t), \boldsymbol{\theta}(t), \boldsymbol{\psi}(t)\right)$ as defined by equation (2) where $\boldsymbol{\varphi}(t) = \boldsymbol{\varphi}\left(\ddot{\boldsymbol{x}}(t), \ddot{\boldsymbol{y}}(t), \ddot{\boldsymbol{z}}(t)\right)$, and $\boldsymbol{\theta}(t) = \boldsymbol{\theta}\left(\ddot{\boldsymbol{x}}(t), \ddot{\boldsymbol{y}}(t), \ddot{\boldsymbol{z}}(t)\right)$, which means $\boldsymbol{\mu}(t) = \boldsymbol{\mu}\left(\ddot{\boldsymbol{\xi}}(t)\right)$. Thus from the torque equation we can conclude $\boldsymbol{\tau_B}(t) = \boldsymbol{\tau_B}\left(\boldsymbol{\xi}^{(4)}\right)$, where $\boldsymbol{\xi}^{(4)} = d^4\boldsymbol{f}(\boldsymbol{t})/dt^4$ is the fourth time derivative of the displacement curve vector function ***f(t)***. This means that we have the body torque being a function of the displacement snap, the fourth time derivative of the displacement. This is the point where [15] draws the conclusion to use minimum snap trajectories.

But this is not the complete picture! For multi rotors the control signal is the angular velocity of the rotor blade, which is not an arbitrary 'just a mathematical' function; it is a real physical system! For BLDC actuators we have $\boldsymbol{i_e}(t) \approx const_2 \cdot \boldsymbol{\tau_{Bi}}(\boldsymbol{\xi}^{(4)})$, so the discontinuity in snap ($\boldsymbol{\xi}^{(4)}$) means a discontinuity in the electric current $\boldsymbol{i_e}(t)$, which is physically not possible. Since the complete electrical equation of an electric motor is:

$$\boldsymbol{v_e}(t) = L_e \frac{d\boldsymbol{i_e}}{dt} + R_e \boldsymbol{i_e}(t) + K_b \boldsymbol{\omega}(t) \tag{3}$$

where the rotation velocity of the rotor is $\boldsymbol{\omega}(t)$; and L_e, R_e are the electrical inductance and resistance of the armature; K_b is the back EMF parameter. The torque equation is:

$$K_\tau \boldsymbol{i_e} - \boldsymbol{\tau_L} = J_M \frac{d\boldsymbol{\omega}}{dt} + \gamma_M \boldsymbol{\omega}. \tag{4}$$

where K_τ is the torque constant; J_m is the motor inertia; and γ_M is the rotor friction coefficient. The motor load torque for a rotor blade application is:

$$\tau_L = J_R \frac{d\omega}{dt} + K_d \omega^2. \tag{5}$$

where K_d is the rotor drag parameter and J_R is the rotor blade inertia. Both, by approaching from the impossibility of the load torque discontinuity or the impossibility of voltage discontinuity we conclude that neither $\frac{d\boldsymbol{\omega}}{dt}$ nor $\frac{d\boldsymbol{i_e}}{dt}$ is allowed to be discontinuous in real life. Further on from equation (4) we have:

$$\frac{d\boldsymbol{i_e}}{dt} = \frac{1}{K_\tau}\left((J_M + J_R) \frac{d^2\boldsymbol{\omega}}{dt^2} + (\gamma_M + 2K_d \boldsymbol{\omega}) \frac{d\boldsymbol{\omega}}{dt} \right), \tag{6}$$

which means that even $\frac{d^2\boldsymbol{\omega}}{dt^2}$ has to be continuous! As $\boldsymbol{\tau_L}$ dominantly depends on $\boldsymbol{\omega}$ ($\boldsymbol{\tau_L} \approx K_d \boldsymbol{\omega}^2$), and we have already concluded that $\boldsymbol{\tau_B}(t) = \boldsymbol{\tau_B}(\boldsymbol{\xi}^{(4)})$, **we can conclude that for a realistic, feasible control input of multi-rotor UAVs the designed path has to be such that the displacement snap ($\boldsymbol{\xi}^{(6)}$) must be continuous and $\boldsymbol{\xi(t)}^{(4)} \sim \boldsymbol{\omega(t)}$!** The major driving force behind the proposal of this paper is that by acknowledging the obligatory physical requirement of the actuator torque and the actuator electric motor current being at least 2 times smooth – so the actuator rotor displacement jerk ($\frac{d^2\boldsymbol{\omega}}{dt^2}$) has no discontinuities: we must respect a physical requirement to have the $\boldsymbol{\xi}(t)$ multi-rotor displacement continuous up to pop, its 6th time derivative $\boldsymbol{\xi}^{(6)}(t) = d^6\boldsymbol{\xi}/dt^6$. Another observation is that since body torques $\boldsymbol{\tau_B}(\boldsymbol{\xi}^{(4)})$ are induced by the combined electric motor torque equations (2), they cannot change at an arbitrary pace, the torque changes must obey the capability of the electric motor in terms of transient behaviour at changing the rotation speed $\tau_B(\boldsymbol{\xi}(\mathrm{t})^{(4)}) \approx K_d \boldsymbol{\omega}^2(t)$.

After algebraic manipulations of equations (3-5) by Laplace transformations we can conclude:

$$I_e = \frac{V_e - K_b W}{R + Ls} \tag{7}$$

by notation $(J_M + J_R) = J, K_T = K_b = K,\ \ B = L_e J, C = R_e J + L_e \gamma_M, D = L_e K_d$ we get:

$$-Bs^2 W - sW(C + DW) = KV_e - W(K^2 + R_e \gamma_M + R_e K_d W), \tag{8}$$

where the right hand side represents the stationary mode of the electric motor, and the left hand side represents the dynamic transient mode. For cases of voltage control we can use directly the solution of equation (8), while for current control of the electric motor, the solution has to be substituted to equation (7). For the stationary case we can directly calculate the required v_e for an arbitrary stationary ω_{stat} by making the transient left hand side equal to zero. The solution of the left hand side, keeping the right hand side zero, defines the transient mode characteristic of the rotation angular velocity $\boldsymbol{\omega_t}(t)$ as:

$$\boldsymbol{\omega_t}(t) = -\frac{C}{D} - (\frac{AB}{D}) tanh(\frac{A}{2}(T_h - t)), \tag{9}$$

where $A = \sqrt{(\frac{C^2}{B^2} + \frac{2D}{B}E)}$, T_h; and E are constants calculated for $\boldsymbol{\omega_t}(0) = \omega_0$, $\dot{\boldsymbol{\omega}}_{\boldsymbol{t}}(0) = \omega_{d0}$ boundary conditions. For $\dot{\boldsymbol{\omega}}_{\boldsymbol{t}}(0) = \omega_{d0} = 0$ equation (9) can be presented in the form of:

$$\boldsymbol{\omega_t}(t) = \frac{\omega_{stat}}{2}\left(1 + tanh\left(\frac{\pi}{P}\left(t - \frac{P}{4}\right)\right)\right), \tag{10}$$

where ω_{stat} stands for the targeted stationary rotation speed; P is a system specific parameter - the settling time of the transient; for the given boundary condition $E = E(\omega_0)$ we have:

$$P = \frac{2\pi}{A} = 2\pi\sqrt{\left(\frac{C^2}{B^2} + \frac{BD}{B^2}E\right)^{-1}} = \frac{2\pi L_e(J_M + J_R)}{\sqrt{(R_e(J_M + J_R) + L_e\gamma_M)^2 + EL_e(J_M + J_R)L_e K_d}} \tag{11}$$

Dependency of multirotor torque and rotor blade angular velocity on the continuity of the pop function can be also demonstrated by simply calculating and plotting these system values for an artificially created step function-like trajectory pop [27] – it is well notable that any discontinuity in the trajectory pop will result in a discontinuity in the time derivative of the required rotor angular velocity, which we have already concluded to be a physical not feasible requirement. Compared to the analysed multi-rotor dynamics (1)-(11), a 3D overhead crane model and a RM dynamics model are of the same basic format as equation (1), but these systems are more simple as the position of the payload or end effector is directly linked to the position of the actuator rotor shaft – there is no intermediate transfer function like equation (2) for a multi-rotor. This fact predicts that cranes and RMs are not sensitive to discontinuities in the trajectory pop or crackle, only the snap has to be continuous.

4 New Energy Efficient, Feasible, Time Optimal Trajectory Design

The important message of the proposal of this paper based on [18] is that we must not overlook the physical capabilities, constraint of neither the system nor the actuator itself. For multi-rotors their body torques and matching rotation speed of rotors and their transient behaviour is limited – these constraints are proportional to properties of the trajectory displacement snap $\boldsymbol{s}(t) = \boldsymbol{\xi}^{(4)}(t)$. The snap is required to be 2 times smooth, equivalent to pop $\boldsymbol{p}(t) = \boldsymbol{\xi}^{(6)}(t)$ being continuous [18], [27]. Also the transient behaviour of rotor $\boldsymbol{\omega_t}(t)$ rotation speed has to be proportional to $1 + tanh\left(\frac{\pi}{P}\left(t - \frac{P}{4}\right)\right)$.

The proposal of this paper is to use for the snap transient a base function in the form of:

$$\boldsymbol{c_t}(t) = \boldsymbol{\xi_t}^{(5)}(t) = G \cdot \left(1 - cos\left(\frac{2\pi}{P} t\right)\right), \tag{12}$$

where P is the design parameter responsible for the trajectory duration and also the energy efficiency with oscillation avoidance, its value has to be equal or an integer multiple of the settling time of the $\boldsymbol{\omega_t}(t)$ actuator system - in case of BLDC see equation (11); and G is the design parameter by which we freely control the required displacement length for traveling any distance. By this we obtain the pop base continuous transient function as:

$$\boldsymbol{p_t}(t) = \boldsymbol{\xi_t}^{(6)}(t) = G \cdot \frac{2\pi}{P} \sin\left(\frac{2\pi}{P} t\right). \tag{13}$$

Notice that for 3D overhead cranes and a RMs it is expected to be enough to have $\boldsymbol{\xi_t}^{(4)}(t) = G \cdot \frac{2\pi}{P} \sin\left(\frac{2\pi}{P} t\right)$, since we have a direct link between the actuator motor shaft position and the system variables $\boldsymbol{q}(t) = \boldsymbol{\xi_t}(t)$ – as opposed to multi-rotors, where equation (2) has to be first applied.

5 New Trajectory Design Algorithm

For any trajectory we have a target position and generally a limit to the maximum velocity $\xi^{(1)} < V_{max}$ for safety. Usually there is also a limit $\left|\xi^{(2)}\right| < A_{max}$ to the acceleration and deceleration, too – either for power source capacity, constructional integrity or passenger well-being reasons. For advanced projects also the jerk is to be limited $\left|\xi^{(3)}\right| < J_{max}$ as it has already been concluded by many researchers either to reduce structural vibrations or just for passenger comfort.

The proposal of this paper is to use for multi-rotors a parameterised single sinus wave $\boldsymbol{p}(t) = G\frac{2\pi}{P}\sin\left(\frac{2\pi}{P}t\right)$ as the base function for the displacement pop to reach the desired smooth crackle as $\boldsymbol{c}(t) = \int \boldsymbol{p}(t)dt = G\left(1 - cos\left(\frac{2\pi}{P}t\right)\right)$, which is of transient characteristics physically feasible to match by a BLDC motor. P is the period of $\boldsymbol{p}(t)$ and by this it must match the dynamics of the actuated system. G can be an arbitrary positive real value, which controls the amplitude of the pop base function and thus trajectory displacement length. The integral of a full period $\boldsymbol{c}(t)$ for $t=1..P$ is to be used for the ascending part of the jerk function $\boldsymbol{j}^{+}(t) = \int \boldsymbol{c}(t)dt$, for simplicity we take *0* for the integral constant value. For $\boldsymbol{j}^{-}(t)$ descending part of jerk the integral of $-\mathbf{c}(t)$ is taken. In case that the acceleration $\boldsymbol{a(t)} = \int\left(\boldsymbol{j}^{+}(t) + \boldsymbol{j}^{-}(t+P)\right)dt$ does not reach the desired level, a constant $\boldsymbol{j_{max}}$ interval is to be inserted between $\boldsymbol{j}^{+}$ and $\boldsymbol{j}^{-}$ intervals. The velocity is planned in an analogous manner, by integrating the rising acceleration and the falling deceleration interval, with optional inclusion of a constant acceleration interval to reach the desired maximum velocity, all this without overshooting the reached acceleration limit. By keeping the velocity constant in the middle of the trajectory we ensure feasible time optimally reaching the desired displacement without exceeding the speed limit.

The algorithm is:

0. Account for all defined limitations in snap, jerk, acceleration, velocity, displacement, duration, for each calculate the boundary consequence on each higher derivative:
   a. *limit_snap* directly limits:
      limit_P=limit_snap/G;
   b. *limit_jerk* limits:
      limit_P=sqrt(limit_jerk/G) and
      *limit_snap=G*limit_P*;
   c. *limit_acceleration* limits:
      *limit_P=nthrooth(limit_acceleration/(2*G),3)* and
      *limit_snap=G*limit_P* and
      limit_jerk=$G*(limit\_P)^2$
   d. *limit_velocity* limits:
      *limit_P=nthrooth(limit_velocity/(8*G),4)* and
      *limit_snap=G*limit_P* and
      limit_jerk=$G*(limit\_P)^2$ and
      limit_acceleration=$G*2*(limit\_P)^3$
   e. *limit_displacement* limits:
      *limit_P=nthrooth(limit_velocity/(64*G),5)* and
      *limit_snap=G*limit_P* and
      limit_jerk=$G*(limit\_P)^2$ and
      limit_acceleration=$G*2*(limit\_P)^3$ and
      limit_ velocity =$G*8*(limit\_P)^4$
   f. *limit_duration* limits:
      limit_P=limit_duration/16

1. select the minimal calculated limit of all above calculated values for each derivative: *limit_P, limit_snap, limit_jerk, limit_acceleration, limit_velocity,* values calculated in step 0.

2. calculate base feasible values:
   base_P = min([limit_P]) from step 1.
   *base_cracle = G*2*
   base_snap = base_P
   *base_jerk = base_snap*base_P*
   *base_acceleration = base_jerk*2*base_P*
   *base_velocity = base_acceleration*4*base_P*
   *base_displacement = base_velocity*8*base_P*
   *base_duration = 16*base_P*

3. select the smallest admissible *allowed_P*, *allowed_snap, allowed_jerk, allowed_acceleration*, *allowed_velocity* from limit and base values calculated in steps 1 and 2.

4. calculate final trajectory parameters
   a. P = allowed_P
   *b. max_cracle = G*2*
   l_cracle = P/2
   *c. max_snap = max_cracle * l_cracle*
   *l_snap = 2 * l_cracle*
   d. increment_jerk = max(0, allowed_jerk/max_snap – l_snap)
   *max_jerk=mas_snap * (l_snap + increment_jerk)*
   *l_jerk=2 * l_snap + increment_jerk*
   e. increment_acceleration=max(0, allowed_acceleration/max_jerk – l_jerk)
   *max_acceleration = max_jerk * (l_jerk + increment_acceleration)*
   *l_acceleration = 2 * l_jerk + increment_acceleration*
   f. increment_velocity = max(0, allowed_velocity/max_acceleration – l_acceleration)
   *max_velocity = max_acceleration * (l_acceleration + increment_velocity)*
   *l_velocity = 2 * l_acceleration + increment_velocity*
   g. increment_displacement = max(0, allolwed_displacement/max_velocity – l_velocity)
   *max_displacement = max_velocity * (l_velocity + increment_displacement)*
   *l_displacement = 2 * l_velocity + increment_displacement*
   h. increment_duration = max(0, target_duration – l_displacement)
   *max_duration = 16 * P + 8 * increment_jerk + 4 * increment_acceleration + 2 * increment_velocity + increment_displacement + increment_duration*

Notice that for numerical robustness in discrete calculations one must take care of each variable *l_#* and *increment_#*, and also values *#_P*, as they have to be integer multiples of the sampling time, otherwise the required exact balance between positive and negative areas of acceleration and higher derivatives cannot be ensured. The discrete algorithm thus cannot generate trajectories to arbitrary displacement with absolute precision. The generated displacement final position error is proportional to *numerical_endposition_error = 16 * P - integer(16 * P / sampling_time) * sampling_time*.

6 New Trajectory Design Algorithm Results for Multi-Rotors

The basic smooth trajectory parametrization curve used in this paper is presented in Figure 2 with sampling time $dt = 0.001$[s]:

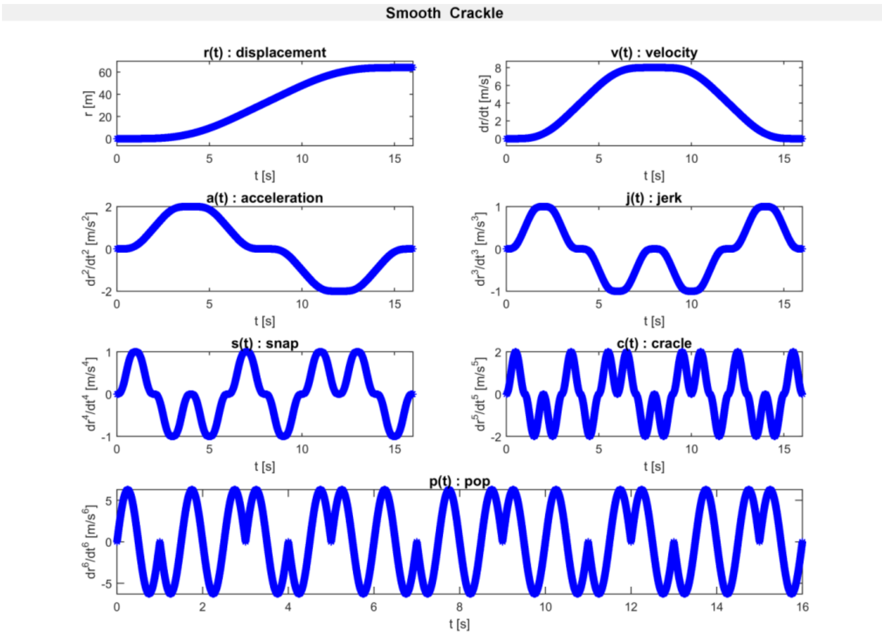

Figure 2

Smooth crackle trajectory components with sinusoid base pop functions

which results in a feasible time optimal trajectory with dynamic boundaries for maximum of *pop* = 2π [m/s^6] sinus wave of 1[s] period, maximum of *crackle* = *2*[m/s^5], *maximum_snap* = *1*[m/s^4], *maximum_jerk* = *1*[m/s^3], *maximum_acceleration* = *2*[m/s^2], *maximum_velocity* = *8*[m/s], *displacement* = *64*[m], for displacement *duration* = *16*[sec]. The integral of absolute jerk is 8[m/s^2], what is proportional to the expended energy (as mass and desired displacement we consider to be constant).

This base trajectory parametrisation is projected to the training path of connecting back and forth the opposite corners ***(x,y,z)*** = *(0,0,0)->(64,64,64),(64,64,64)->(0,0,0)* of a 64m cube, while performing simultaneous a full jaw rotations in each direction $\boldsymbol{\psi}$ = *(0->2π),(2π->0)*.This results in training data worth of 34 seconds of flight time. For the general case of *P=1* trajectory plots and corresponding smooth UAV body torques are:

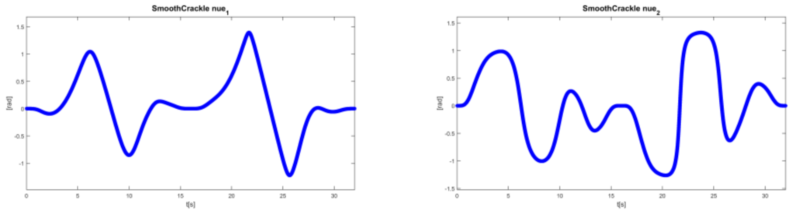

Figure 3

The new continuous crackle trajectory – UAV smooth body roll $\phi(t)$ and pitch $\theta(t)$

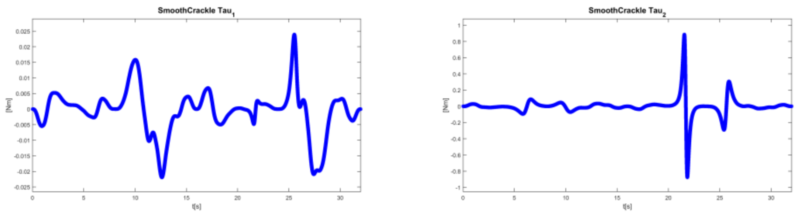

Figure 4

The new continuous crackle trajectory – UAV smooth body torques τ_1, τ_2

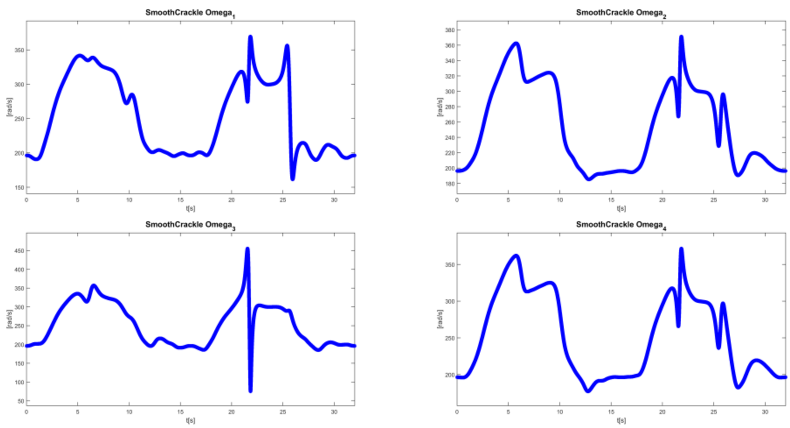

Figure 5

The new continuous crackle trajectory – UAV rotor blades' smooth angular velocity

7 New Trajectory Design Algorithm Applicability to Other Systems

The generated trajectory can be applied as parametrisation to any vector function defined path $\boldsymbol{f}(t)=(\boldsymbol{f}_x(\boldsymbol{r}(t)),\boldsymbol{f}_y(\boldsymbol{r}(t)),\boldsymbol{f}_z(\boldsymbol{r}(t)))$. When determining the constraints on trajectory derivatives, one has to take into consideration both the system limits and curvature properties of the desired path $\boldsymbol{f}(t)$ and its derivatives. $\boldsymbol{f}(t)$ has to be smooth at least up to the required smoothness of the trajectory.

Reduction of the method is strait forward to systems with simpler trajectory constraints, like RMs or wheeled vehicles, where it is enough to have smooth trajectories up to the 3rd time derivative of displacement. A 3D crane, as described in [3] is a simple system, which can in a feed forward control setup very notably present system oscillations induced by the prescribed trajectory. Figure 6 presents the crane system feed forward output error (payload delta position and pitch angle) for a bang-bang acceleration and for a minimal torque, aka. minimal electric energy trajectory; the dimensionless cost function $\boldsymbol{C_{el}}(s) = \frac{1}{2}\int_0^{t_f}(\ddot{\boldsymbol{r}}(t)^2 + \dot{\boldsymbol{r}}(t)^2 + \boldsymbol{r}(t)^2)dt$ was minimised by calculus of variation, where $r(t)$ is the displacement.

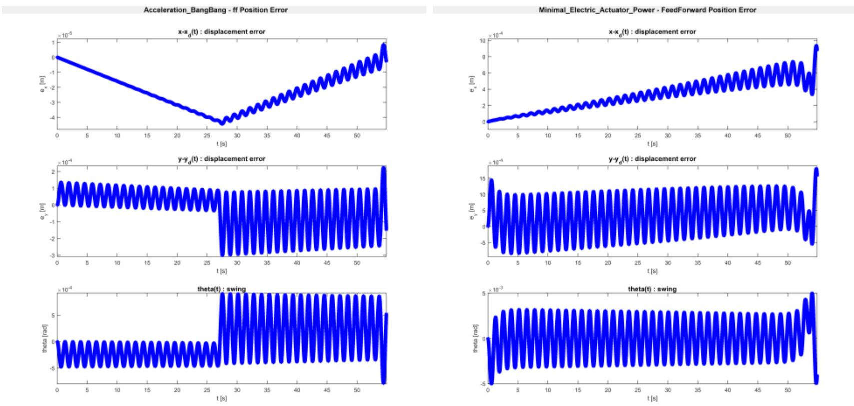

Figure 6

Crane feed forward response error: bang-bang acceleration; and minimal torque trajectory

Table 1. presents the numerical results for maximum payload pitch (Theta), maximum payload tracking error along x and y, and the torque cost (electric energy cost function) for classical optimal trajectories. Table 2. presents the numerical results for the proposed smoot trajectories, measured by the same objective functions.

One can conclude by looking at the numerical results of 'hastier trajectories' in Table 1 that the more timid, slower changing the trajectory is, the better the performance is along all for objectives. The "w_0" reference in the table stands for the used ideal pendulum angular frequency $\omega_0 = \sqrt{g/L}$, where g is the gravity acceleration (9.81m/s^2) and L is the pendulum length; the divisor "w_0/n" by the angular frequency in the trajectory name represents the trajectory length multiplier compared to a smooth trajectory defined by a pop base function of period ω_0 (a trajectory of name ending with "w0/2k" takes 2 times longer to complete than that of "w0/k").

Table 1

Numerical results for the crane feed forward control setup

TRAJECTORY TYPE / PERFORMANCE	***maxTheta***	***maxErrorX***	***maxErrorY***	***maxTorqueCost***
Minimal_Jerk w0:	3.72E-04	3.73E-05	1.21E-04	1.25E-01
Acceler_BangBang w0:	9.04E-04	4.44E-05	3.00E-04	1.34E-01
Minimal_Snap w0:	4.76E-04	4.35E-05	1.53E-04	1.48E-01
Minimal_Crackle w0:	6.01E-04	4.90E-05	1.89E-04	1.67E-01
Minimal_Torque w0:	5.02E-03	9.35E-04	1.80E-03	7.24E-02
Minimal_Acceler w0:	7.07E-04	8.97E-05	2.29E-04	9.96E-02
Vmax_Lightning w0:	2.50E+00	1.58E+01	1.58E+01	1.94E+03
HASTIER TRAJECTORIES:				
Minimal_Torque w0*2:	1.05E-02	1.88E-03	3.01E-03	1.57E-01
Minimal_Torque w0*4:	2.28E-02	2.14E-03	6.55E-03	3.63E-01
Minimal_Torque w0*8:	6.56E-02	5.77E-03	1.59E-02	9.09E-01
Minimal_Torque w0*16:	2.88E-01	2.35E-02	6.40E-02	2.73E+00
Minimal_Torque w0*32:	7.97E-01	7.84E-02	1.30E-01	6.43E+00
SMOOTH TRAJECTORIES:				
SmoothCrackle_w0/32:	1.93E-06	1.51E-06	1.70E-06	8.18E-03
SmoothSnap_w0/16:	7.74E-06	3.01E-06	4.30E-06	1.64E-02
SmoothCrackle_w0/16:	7.74E-06	3.01E-06	4.31E-06	1.64E-02
SmoothSnap_w0/8:	3.11E-05	6.03E-06	1.28E-05	3.31E-02
SmoothCrackle_w0/8:	3.11E-05	6.03E-06	1.28E-05	3.31E-02
SmoothSnap_w0/4:	1.26E-04	1.21E-05	4.33E-05	6.73E-02
SmoothCrackle_w0/4:	1.26E-04	1.21E-05	4.34E-05	6.73E-02
SmoothSnap_w0/2:	5.33E-04	2.42E-05	1.65E-04	1.39E-01
SmoothCrackle_w0/2:	5.33E-04	2.43E-05	1.65E-04	1.39E-01
SmoothSnap_w0:	2.51E-03	1.04E-04	7.04E-04	2.95E-01
SmoothCrackle_w0:	2.53E-03	1.05E-04	7.08E-04	2.95E-01

All trajectories planned for faster completion than $t_T = 2 * \pi/\omega_0$ end up with oscillations. The proposed smooth trajectories are always inducing less oscillation than the classical "minimum" counterparts. The minimum crackle and the proposed smooth crackle trajectories are the only two trajectory types that starting from $t_T = 2 * \pi/\omega_0$ long trajectory motions, which result in no significant crane pendulum second state derivative oscillations. For longer durations other variants of the proposed smooth trajectories are totally vibration free. One benefit of the proposed smooth trajectory is in the designed, arbitrary bounded derivative maximum values – one can set any velocity, acceleration, jerk, even snap limits. The other benefit is that by increasing the level of smoothness one can ensure absolute oscillation free behaviour and reduce the position error, even to reduce the required energy – of course all this is at the cost of longer trajectory durations.

Figure 7 presents crane system second time derivative state oscillations induced by different trajectories; for the maximum velocity and the acceleration bang-bang there is just no point in looking at the second time derivative of the y position, only the position and its first derivative is presented, respectively. Notice that for this crane system example an incomplete mathematical model is used as in [3] – it does not include the actuator dynamics – it counts with the control signal being of arbitrary precision simple mathematical function. For this research paper I have not compensated this model deficiency, so that my results can be directly compared to [3].

The same basic principle of accounting for system oscillations and the actuator dynamics when planning for system trajectories can be also applied to this crane model and any other than electro motor actuated system, by replacing equations (3) to appropriate ones, and then evaluating their transient behaviour. When the actuator dynamics and its relation to the system trajectory is known, one can use the algorithm and the method described in this paper to design trajectories of required transient dynamics and smoothness by replacing equation (4) to the appropriate one [18].

Conclusions

This paper presents a novel direct path construction algorithm based on [18] for generating physically feasible, time-and energy optimal, bounded, continuous trajectories that can reach any target displacement with a known minimal error. These trajectories can be designed to arbitrary smoothness – depending on system requirements; they are to be designed smooth up to the 5^{th} time derivative of displacement for multi-rotor UAV trajectories, as introduced in [18], [19] and used for multi-rotor UAV genetic fuzzy system identifications in [20], [21], [22].

The proposed trajectory design method is capable of forming bounded, smooth, energy efficient and time optimal trajectories with a single pass algorithm using closed formulas [18]. The notion of time and energy optimality is not used in a mathematics theory manner but in real life physically feasible engineering manner. The design method is defined and validated on an example for a multi-rotor UAV path planning, where a single parameter controls the trajectory dynamics.

The proposed trajectory design method results in real-life feasible smooth, limited torque transients that is energy efficient for control signal design; while providing a flexible interface to arbitrary velocity, acceleration, jerk, snap limit enforcement.

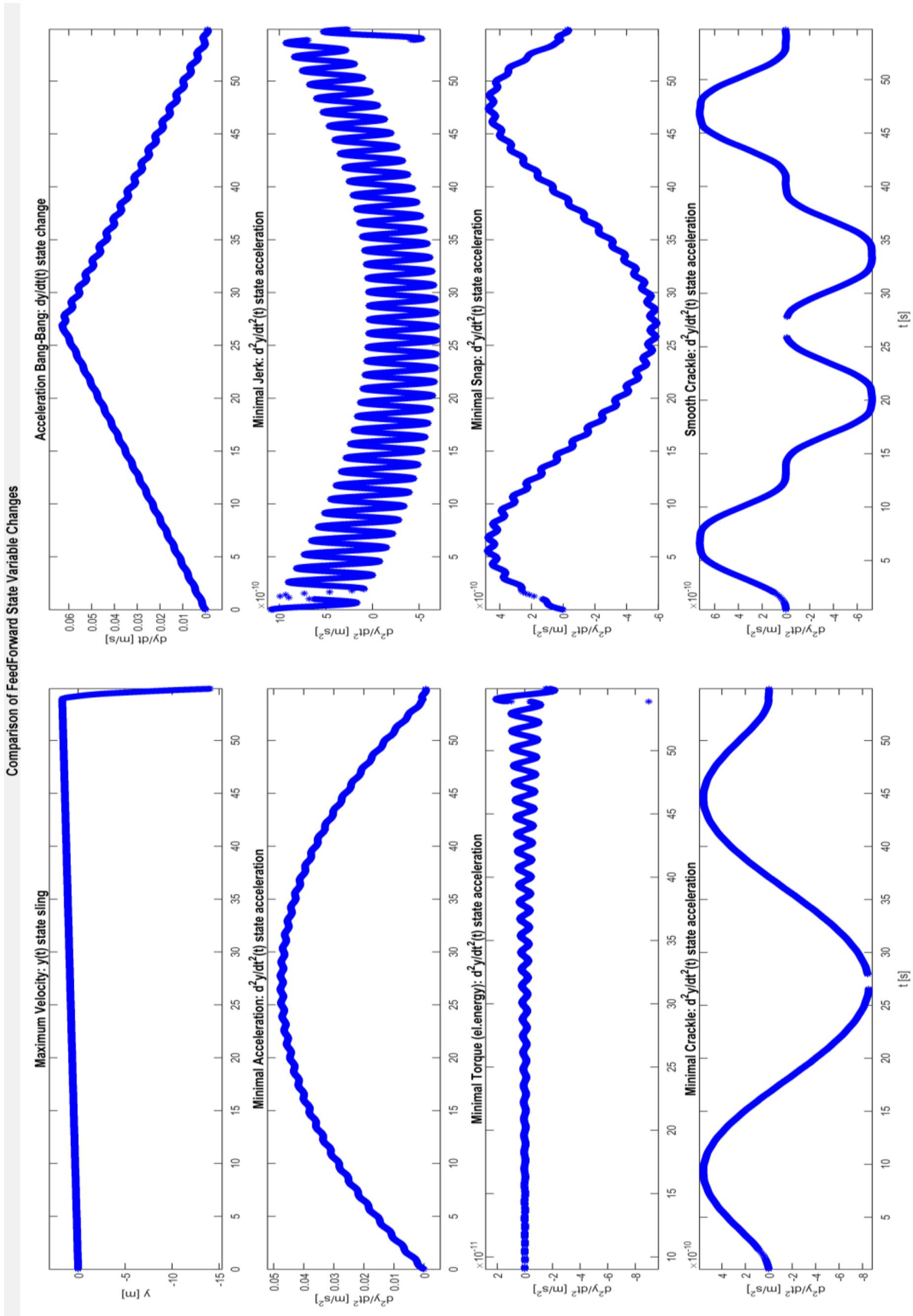

Figure 7

Crane feed forward system's second time derivative of the y state variable for various trajectories

Dynamic transient properties and energy efficiency of the trajectory can be achieved with a single parameter, while the feasibility of torque transients is maintained. The resulting trajectory for the properly selected transient parameter is always the time optimal feasible solution, which complies with all defined limits.

Oscillations reduction, even no oscillation trajectories can be achieved by increasing the trajectory time, which is equivalent to planning with sinusoid pop base functions of 2^n integer multiples of its parameter P. For a 3D overhead crane the no oscillations trajectories require the seventh time derivative $\xi^{(7)}$ of crane displacement to be periodic in sync with the crane's pendulum angular frequency ω_0, while it is already admissible to have discontinuities in the crackle $\xi^{(5)}$, the fifth time derivative of the displacement, when only the acceleration $\xi^{(2)}$ is actually periodic, with $\omega_0/32$.

Generated trajectories, even those of prolonged duration will require less torque, less aggregated actuator energy than the so called energy optimal trajectory – the explanation is that the theoretical "energy optimal" trajectory is a direct calculation of the trajectory acceleration and velocity, opposed to the measured system output, where the used energy is actually the system output based on parameterisation by the trajectory. So though the "energy optimal" trajectory acceleration matches the first component of the actuator power applied in a system feed forward control setup, but the theoretical optimisation process relies on the "energy optimal" trajectory velocity, while in a control setup the velocity/potential energy is actually equal to the resulting system state driven by the control signal (the desired acceleration) – and there can be system control signals, which by itself are more costly than the "energy optimal" trajectory acceleration, but this control signal can drive the system through states, which match to lesser aggregated energy states than the "energy optimal" trajectory velocity indicates by itself. The main reason for this is that the "energy optimal" trajectory induces oscillations, while sufficiently smooth trajectories do not induce vibrations.

Further research should prove the energy efficiency, feasible optimality of these smooth trajectories in a feedback loop. It would also be interesting to find an explanation to the question: why does the no oscillations trajectory require the seventh time derivative $\xi^{(7)}$ of crane displacement to be periodic in sync with the crane's pendulum angular frequency ω_0, while it is already admissible to have discontinuities in the crackle $\xi^{(5)}$, the fifth time derivative of the displacement, when only the acceleration $\xi^{(2)}$ is actually periodic with $\omega_0/32$?

References

[1] A. Nemes: Synopsis of Soft Computing Techniques Used in Quadrotor UAV Modelling and Control, Interdisciplinary Description of Complex Systems, Vol.13, No.1, pp.15-25, 2015.

[2] A.Rodić, G.Mester, I.Stojković: Qualitative Evaluation of Flight Controller Performances for Autonomous Quadrotors, in Intelligent Systems: Models and Applications, Vol.3. Springer-Verlag, Berlin Heidelberg, 2013.

[3] D. Chwa: Nonlinear Tracking Control of 3-D Overhead Cranes Against the Initial Swing Angle and the Variation of Payload Weight, IEEE Transactions on Control Systems Technology, Vol.17, Issue: 4, 2009

[4] N. Varminska, D. Chablat: Optimal Motion of Flexible Objects with Oscillations Elimination at the Final Point, Eucomes, Springer, 2016.

[5] L.S. Pontryagin, V.G. Boltyanskii, R.V. Gamkrelidze, E.F. Mishchenko: The mathematical theory of optimal processes, Interscience Publishers, New York, 1962.

[6] J.T. Betts: A survey of Numerical Methods for Trajectory Optimization, Mathematics and Engineering Analysis, Boeing Information and Support Services, Washington, 1998.

[7] R. Zwahlen, T. Chang: Feedforward Speed Control of Brushless DC Motors with Input Shaping, The 33rd Annual Conference of the IEEE Industrial Electronics Society (IECON), Taipei, 2007.

[8] M. Murugan, R. Jeyabharath, P. Veena: Stability Analysis of BLDC Motor Drive based on Input Shaping, International Journal of Engineering and Technology, Vol.5, No.2, pp.1169-1177, 2013.

[9] G. Venu, Dr. S. T. Kalyani: A New Topology for Speed control of Sensor less BLDC Motor with Reduced Commutator Switches and Improved Input Power Factor, International Journal Of Engineering And Computer Science, Vol.3, No.11, pp. 9243-9247, 2014.

[10] J.E. Bobrow, S. Dubowsky, J.S. Gibson: Time-optimal control of robotic manipulators along specified paths, Int. J. Robotic Research, 4(3), 1985.

[11] Y. Bouktri, M. Haddad, T. Chettibi: Trajectory planning for quadrotor helicopter, 16th Mediterranean Conference on Control and Automation, Ajaccio, 2008.

[12] A. Naghash, M. Naghshineh, A. Honari: Minimum Time Trajectory Optimisation for Flying a Quadrotor in an 8-shaped Path, International Micro Air Vehicle Conference and Flight Competition (IMAV2013), Toulouse, 2013.

[13] A. Sanchez, V. Parra-Vega, O. Garcia, F. Ruiz-Sanchez, L. E. Ramos-Velasco: Time-Parametrization Control of Quadrotors with a Robust Quaternion-based Sliding Mode Controller for Aggressive Maneuvering, European Control Conference (ECC), Zürich, 2013.

[14] M. A. Olivares-Mendez, I. F. Mondragón, P. Campoy, L. Mejías, C. Martinezm: Aerial Object Following Using Visual Fuzzy Servoing, in Proceedings of the 1st Workshop on Research, Development and Education

on Unmanned Aerial Systems (REDUAS 2011), Centro Avanzado de Tecnologías Aeroespaciales (CATEC), Seville, Spain, pp. 61-70, 2011.

[15] T. Fraichard A. Scheuer: From Reeds and Shepp's to continuous-curvature paths, IEEE Trans. on Robotics and Automation, 20(6):1025–1035, 2004.

[16] R. Lozano: Unmanned Aerial Vehicles, ISTE Ltd, London, 2010.

[17] D. Mellinger, V. Kumar: Minimum snap trajectory generation and control for quadrotors, IEEE International Conference on Robotics and Automation (ICRA2011), pp. 2520 –2525, 2011.

[18] A. Nemes: Continuous Periodic Fuzzy Logic Systems and Smooth Trajectory Planning for Multi-Rotor Dynamic Modeling, Acta Polytechncia Hungarica, 2016, in press.

[19] A. Nemes: Fuzzy-Genetic Control of Quadrotors Unmanned Aerial Vehicles, Interdisciplinary Description of Complex Systems, 14(2), 2016.

[20] A. Nemes: Genetic Algorithm-Based Adaptive Fuzzy Logic Systems for Dynamic Modeling of Quadrotors, Proceedings of the 3rd International Conference MechEdu, pp.96-103 Subotica, 2015.

[21] A. Nemes: Genetic Fuzzy Identification Method for Quadrotor UAVs, Annals of Faculty of Hunedoara – International Journal of Engineering, Tome XIII, Fascicule 3, pp. 257-264, 2015.

[22] A. Nemes, G. Mester: Unconstrained Evolutionary and Gradient Descent-Based Tuning of Fuzzy partitions for UAV Dynamic Modeling, FME TRANSACTIONS, Vol.45, No.1, pp.1-8, paper No: 16 – 136, 2017

[23] C. Richter, A. Bry, N. Roy: Polynomial Trajectory Planning for Quadrotor Flight, Proceedings of the International Symposium of Robotics Research (ISRR), 2013.

[24] A. Nemes, B. Lantos: Genetic Algorithms-Based Fuzzy Logic Systems for Dynamic Modeling of Robots, Periodica Polytechnica Electrical Engineering, Vol. 43, No. 3, pp.177-187, 1999.

[25] A. Nemes, B. Lantos: Optimization of Fuzzy Logic Systems for Gray-Box Dynamic Modeling of Robot Manipulators by Genetic Algorithms, Proceedings of IEEE INES'99. pp. 353-358, 1999.

[26] A. Nemes, B. Lantos: Training Data Reduction for Optimisation of Fuzzy Logic Systems for Dynamic Modelling of Robot Manipulators by Genetic Algorithms, Proceedings of IEEE Instrumentation and Measurement Technology Conference, Vol.3, pp. 1418-1423, 2001.

[27] A. Nemes, G. Mester: Energy Efficient Feasible Autonomous Multi-Rotor Unmanned Aerial Vehicles Trajectories, Proceedings of the 4th International Scientific Conference on Advances in Mechanical Engineering (ISCAME), Hungary, 2016

[28] G. Mester: Distance Learning in Robotics, Proceedings of The Third International Conference on Informatics, Educational Technology and New Media in Education, pp.239-245, Sombor, 2006.

[29] G. Mester: Improving the Mobile Robot Control in Unknown Environments, Proceedings of the Conference YUINFO' 2007, pp. 1-5, Kopaonik, 2007.

[30] G. Mester, A. Rodic: Modeling and Navigation of an Autonomous Quad-Rotor Helicopter, E-society Journal: Research and Applications, Vol.3, No.1, pp.45-53, 2012.

[31] G. Mester, A. Rodic: Navigation of an Autonomous Outdoor Quadrotor Helicopter, 2nd Int. Conference on Internet Society Technology and Management, pp. 259-262, Kopaonik, 2012.

[32] G. Mester, A. Rodic, J. Stepanic: Nonlinear Control of Aerial Robotics, Modern Approach to Product Development and Business Improvement, Balatonfüred, 2013.

[33] G. Mester, A. Rodic: Négyrotoros robothelikopter modellje és írányítása, A Magyar Tudomány Napja a Délvidéken, Vajdasági Magyar Tudományos Társaság, Újvidék, pp.469-476, 2013.

[34] G. Mester, A. Rodic: Simulation of Quad-rotor Flight Dynamics for the Analysis of Control, Spatial Navigation and Obstacle Avoidance, Proceedings of the 3rd International Workshop on Advanced Computational Intelligence and Intelligent Informatics, pp.1-4, Shanghai, 2013.

[35] G. Mester: Backstepping Control for Hexa-Rotor Microcopter, Acta Technica Corviniensis – Bulletin of Engineering, Tome VIII, Fascicule 3. pp. 121-125, 2015.

[36] G. Mester: Modeling of Autonomous Hexa-Rotor Microcopter, Proc. of the 3rd Int. Conference and Workshop Mechatronics in Practice and Education, pp.88-91, Subotica, 2015.

[37] A. Rodić, G. Mester: Modeling and Simulation of Quad-Rotor Dynamics and Spatial Navigation, Proceedings of the SISY 2011, 9th IEEE International Symposium on Intelligent Systems and Informatics, pp.23-28, Subotica, 2011.

[38] A. Rodić, G. Mester: Remotely Controlled Ground-Aerial Robot-Sensor Network for 3D Environmental Surveillance and Monitoring, invited talk, TAMOP 422 Workshop, Szeged, 2011.

[39] A. Rodić, G. Mester: The Modeling and Simulation of an Autonomous Quadrotor Microcopter in a Virtual Outdoor Scenario, in Acta Polytechnica Hungarica, Vol. 8, No. 4, 2011, pp. 107-122

[40] A. Rodić, G. Mester: Control of a Quadrotor Flight, Proceedings of the ICIST Conference, pp.61-66, Kopaonik, 2013.

[41] Gyula Mester, Distance Learning in Robotics, Proceedings of The Third International Conference on Informatics, Educational Technology and New Media in Education, pp. 239-245, ISBN 86-83097-51-X, Sombor, Serbia and Montenegro, 01-02.04.2006.

[42] Gyula Mester, Pletl Szilveszter, Gizella Pajor, Djuro Basic: Adaptive Control of Rigid-Link Flexible-Joint Robots. Proceedings of 3rd International Workshop of Advanced Motion Control, pp. 593-602, Berkeley, USA, March 20-23, 1994.

[43] Gyula Mester, Neuro-Fuzzy-Genetic Controller Design for Robot Manipulators, Proceedings of the IEEE IECON'95, International Conference on Industrial Electronics, Control and Instrumentation, Orlando, Vol. 1, pp. 87-92, DOI 10.1109/ IECON.1995.483338, ISBN 0-7803-3026-9, Florida, USA, November 6-10, 1995.

[44] Gyula Mester, Neuro-Fuzzy-Genetic Trajectory Tracking Control of Flexible Joint robots. Proceedings of the I ECPD International Conference on Advanced Robotics and Intelligent Automation, pp. 93-98, Athens, Greece, September 6-8, 1995.